# Mechanical behavior characterization of planar and non-planar sandwich composite panels with agglomerated cork core Experimental and numerical study

Nuno Maia de Carvalhal Soares
nuno.soares@ist.utl.pt

Instituto Superior Técnico, Universidade de Lisboa, Portugal
March 2017

---

**Abstract:** This paper presents an experimental and numerical study on the mechanical behavior analysis of laminated sandwich composites, with an agglomerated cork core reinforced with fiber glass and epoxy resin skins. Planar and non-planar panels are analysed and a comparison between their behavior under compression is performed, whereas a specific configuration based on the DesAIR project was used. Tensile and compression experimental tests were first performed to determine the mechanical properties of the skins and of the core material, which were then compared with the analytical solution. The orthotropy and the transversal isotropy of the skins were verified, as well as the isotropy of the core. Planar and non-planar panels were experimentally tested, from which the load-displacement curve was taken. A numerical model was developed for the compression test and for both panels. The previously determined properties for the skins and for the core were inserted on the numerical model, the finite elements analysis was performed and the results were obtained. Convergence was achieved. Through the comparison of the experimental load-displacement curve with the numerical, one can conclude that the achieved numerical model is valid for this type of test and for both panels, considering small displacements. For larger displacements, non-linear effects are dominant. The resin impregnation amongst the cork cells and the warp of the panels are some of the factors that introduce differences. Improvements on the hand lay-up method, on the analysis with the VIC and on the hyperelastic model that simulates the cellular behavior of the agglomerated cork core are suggested. However, results show great potential for the creation of numerical models to characterize sandwich structures with cellular and non-linear cores.

**Keywords:** laminated sandwich composites, planar and curved panels, agglomerated cork core, mechanical behavior, compression, finite elements analysis.

---

## 1. Introduction

Humanity always had the need to improve the characteristics of the materials that were provided by nature and freely available in the environment. Nowadays, composite materials have had an extreme development and the search for new and improved composites is still one of the main quests in engineering, mainly due to their ability of improving needed mechanical properties while accurately decreasing weight. Lightweight but stronger materials are one of the main requisites for the aerospace industry, for example, which saw a major development since the First World War.

With the current technology, composites can be shaped into almost any desired design, which opens the possibilities up to a completely new set of non-linear and dynamic shapes, that can be used to make the final products more or less aerodynamic, aeroelastic, etc. In addition, research is being conducted on the usage of new materials, which were never used before for this purpose and that have special characteristics for the needed applications, such as natural materials. For example, cork, when used as a core on a sandwich composite and when reinforced with for example glass fibers, presents several enviable properties, due to its cellular structure. Thus, the usage of cellular materials on composite structures also undertakes improved environmental performance, which is the key towards a sustainable future. Cellular materials, like cork, are expected to be used on the aerospace field as a substitute to the materials that are conventionally used as cores of sandwich panels, such as foams and aluminium honeycombs.

The sandwich structure chosen for this research work has an agglomerated cork core reinforced with fiberglass and epoxy resin skins. So, being this sandwich configuration a rather new one and currently still under development, its mechanical behavior is not yet fully characterized nor easily available, such as it is for most metals, for example. Thus, experimental and numerical studies must be conducted to proper characterize the sandwich's materials, because they dictate

ultimately in which way it could be used for a given application. Also, the main type of structure to be analysed is a rather innovative one, which is a non-planar or curved panel. Thus, when one combines the analysis of a non-linear material, such as agglomerated cork is, with the analysis of a sandwich which has this material as core and, ultimately, with the analysis of this structure as a non-planar one, several innovative aspects are being addressed simultaneously, which might place this study as one of extreme relevancy.

The type of sandwich composite structure object of the present dissertation, falls within the framework of the DesAIR Project, which is the result of a consortium of several entities: Almadesign, Amorim Cork Composites, Frontwave, Embraer, Couro Azul, INEGI and the University of Beira Interior UBI. Therefore, this study also provided the author with the opportunity to be part of this project and to be in contact with several companies. Besides the stated, the motivations for this study fall on the innovative character inherent to this recent topic, as well as on the imminent future work that could be still further developed. Ultimately, the author hopes to awake the curiosity of the scientific community towards the several applications of this sandwich structure on the field of engineering and, particularly, on aerospace engineering.

## 2. Background

The author gives a review on cork, its structure and its mechanical behavior. The preliminary design is given considering the DesAIR Project.

### 2.1. Cork

Cork is a natural material obtained from the Quercus suber L. oak tree [1]. The first time that cork's microscopic structure was observed was by Robert Hooke in the XVII century [2]. However, only with the scanning electron microscope (SEM), its full microscopic structure and mechanical behavior could be understand. Cork possesses an alveolar structure of closed cells with no empty spaces between them, like a honeycomb [1]. Cork cells can be from straight to heavily corrugated or even collapsed, which might result from compression during cellular growth. The later the cork is, the thicker and stronger the cell walls are, which means that much less corrugation exists [3]. Cork cells are closed and hollow, with very thin membranes filled with a large quantity of a gas, presumably similar to air [4], which leads to a very low specific weight.

### 2.2. Mechanical properties

Cork mechanical properties are quite unique. When compressed (*Figure 1*), the obtained cork stress-strain curve exhibits three different zones, typical from flexible cellular materials and, when tensioned (*Figure 2*), the curve exhibits a similar behavior for all the three directions [1].

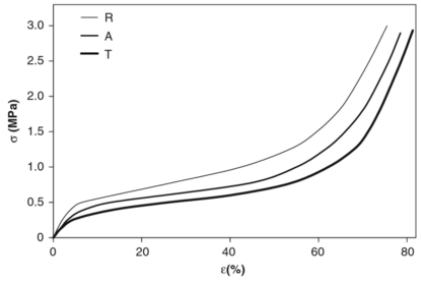


*Figure 1: Stress-strain curve obtained for boiled cork along all directions and for a compression test [5].*

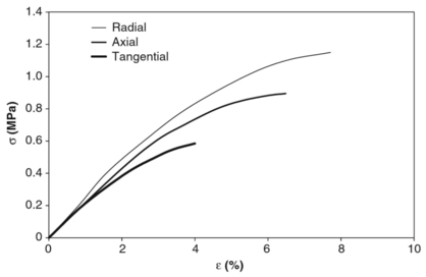


*Figure 2: Stress-strain curve obtained for boiled cork along all directions and for a tensile test [5].*

When compressed, different effects occur. For the radial direction, the cell walls fold, corrugations increase and the cell bases align, which turns the Poisson's coefficient into a small positive value, due to the expansion in the non-radial directions. For the tangential and axial directions, the cell walls bend and straighten, the undulation pattern changes and a negative Poisson's coefficient is obtained, due to shrinking in the radial direction.

### 2.3. The DesAIR Project

DesAIR is a project that was officially presented on April 2015 and whose aim is to develop new high performance composite solutions for aircraft interiors, with a wide range of applications and integrating natural materials through the development of specific manufacturing processes [6]. Thus, one of its main objectives is the mechanical behavior analysis of the non-planar panels that are part of the structure. Therefore, the panel highlighted on *Figure 3* was selected and two considerations were taken: the panel's dimensions were reduced on a 1:3 scale, due to the testing machine dimensions; and, since the non-planar panel is curved multiple times in different axes, only the main curvature was considered.

*Figure 3: DesAIR Project and the given curved panel [6].*

## 3. Experimental study

For the panel's experimental compression test, 6 specimens were produced (3 of flat and 3 of curved panels) based on the DesAIR's Project dimensions at a 1:3 reduced scale (*Figure 4*). For further notice, the relationship between the structural axes and the material axes is: the tangential direction is number 1, the axial direction is number 2 and the radial direction is number 3.

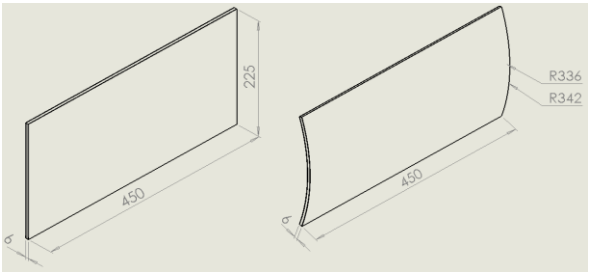


*Figure 4: Flat panel (left) and curved panel (right) dimensions. From the total thickness of 6 mm, 5 mm correspond the core and the other two 0.5 mm correspond to each one of the two skins.*

### 3.1. Mechanical properties

Since the properties of the materials were needed for the development of the numerical model, tests must be performed. The characterization tests for the materials comprised a total of 66 specimens, from which 28 were tested to determine the properties of the skins material and 38 were tested to determine the properties of the core material.

#### 3.1.1. Determination of the skins properties

The skins of the sandwich composite, since they consist of bidirectional 300 g/m² glass fibers impregnated in epoxy resin and hardener 1050/1058S, are orthotropic and elastic. So, for the obtainence of the skins properties, the theory for an orthotropic material was reviewed from reference [7] and from pages 26-31. The needed nine independent material coefficients for an orthotropic material are $E_1$, $E_2$, $E_3$, $G_{23}$, $G_{13}$, $G_{12}$, $\nu_{12}$, $\nu_{13}$, $\nu_{23}$. For the radial direction, which corresponds to the thickness dimension, the fibers effect can be neglected, meaning that the epoxy resin and hardener 1050/1058S properties can be inserted from the manufacturer sheets [8]. However, for the other two directions, the fibers effect cannot be neglected and the previous approximation is no longer valid. Thus, specimens of the skins material were created with the dimensions of *Figure 5* and the properties were experimentally determined according to *Table 1*.

For the analytical properties, the data provided by the manufacturers was considered [8] [9] [10]. Since an axially loaded slender bar is considered, Hooke's Law is satisfied until the elastic limit of the material is reached. The material is considered as both homogeneous and isotropic, i.e., its mechanical properties are independent of position and direction. So, for any transverse direction, the strains have the same value. From equations of pages 86-89 of reference [7] the desired analytical properties are calculated (*Table 2*).

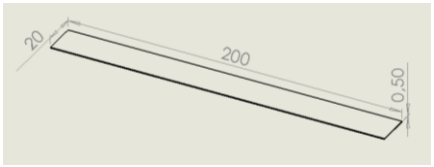


*Figure 5: Specimen's dimensions (in mm).*

*Table 1: Standards for the tests using the skin's material.*

| Test method | Teste Type | Equation |
|---|---|---|
| ASTM D3039/D3039M | Tensile | $\sigma_x = E_x \varepsilon_{xx}$ |
| ASTM D3039/D3039M | Tensile | $\varepsilon_{yy} = -\nu_{xy} \varepsilon_{xx}$ |
| 10º Off-axis Tensile Test | Tensile | $\tau_{10º} = G_{xy} \gamma_{10º}$ |

*Figure 6: Specimen during (left) and after (right) the tensile test.*

For the experimental properties, experimental tests were performed on an INSTRON machine at 2mm/min, while the strains were measured with the VIC 2D (*Figure 6*). So, the specimens were coloured with a black dot's pattern over a white background. After the tests were performed, the results were correlated using a routine in Python and from which the experimental curves were obtained. Through a linear regression on each, the mean of the values obtained for the slope are the desired experimental properties (*Table 2*).

So, one might conclude that the relative error of the obtained properties is as high as circa 45% for

*Table 2: Analytical and experimental skins properties obtained for the numerical model. The values for $E_3$, $\nu_{13}$, $\nu_{23}$, $G_{13}$ and $G_{23}$ were not determined and the resin properties were directly inserted.*

| | $E_1$ [$MPa$] | $E_2$ [$MPa$] | $E_3$ [$MPa$] | $\nu_{12}$ [ ] | $\nu_{13}$ [ ] | $\nu_{23}$ [ ] | $G_{12}$ [$MPa$] | $G_{13}$ [$MPa$] | $G_{23}$ [$MPa$] |
|---|---|---|---|---|---|---|---|---|---|
| Analytical | 16 533 | 16 533 | 3 460 | 0.284 | 0.3 | 0.3 | 1 582 | 1 331 | 1 331 |
| Experimental | 9 852 | 9 042 | 3 460 | 0.192 | 0.3 | 0.3 | 1 878 | 1 331 | 1 331 |
| Relative Error [%] | 40.41 | 45.30 | - | 32.39 | - | - | 18.71 | - | - |

the $E_2$ value. The relatively high relative error's values, which arise when the experimental properties are compared with the analytical and using the last ones as reference, are essentially due to the way in which the VIC 2D calculates the mean strains. The strain values on both the direction of loading and on the transverse direction might be somewhat noisy, and this will have a major effect on the determined properties.

These discrepancies are due to three relevant factors. The first factor is the images being too bright, which makes most of the image overdriven and very little detail in the speckles. The ideal image should have a background with a nice range of grey. The second factor is the variation of the pattern, in which some speckles might be very big and the other ones very small. The big speckles are okay, but the small ones (from one to two pixels) might cause aliasing effects. Finally, the third factor is the waviness of the strains plot. This is normally caused by the existence of refractive heat waves during the test, which might have been caused by the light used. This light, when it is hot, causes index of refraction changes in the air in the optical path, which might also lead to uncertainties on the final obtained result. Even though these factors were minimized, their effect was present.

Therefore, the fairly small strains measured were probably blurred by the three referred factors, which led to the differences between the experimental and the analytical values. Although the relative error is relatively high, both the analytically and the experimentally determined properties for the skins were introduced on the numerical model. The results that will be presented further on the finite elements analysis (FEA) will consider always both properties.

### 3.1.2. Determination of the core properties

The core of the sandwich composite consists in a NL20® cork agglomerate with 5 mm thickness. According to the production of agglomerated cork, cork planks are aleatorily laid, compacted and impregnated with resin. So, since the granules are oriented towards aleatory and different directions, the core will have properties that are similar along the three-orthogonal axis of symmetry. Thus, the core material is isotropic and hyperelastic, due to the cellular nature of the cork itself. However, this hyperelasticity is just evident under compression (*Figure 1*), because under tension its behavior is mainly elastic (*Figure 2*). The two previous figures are the only available analytical results.

For simulation purposes, the only thing that is needed is the complete stress-strain curve of the material. For the verification of the isotropy, the specimens were tested along the three-orthogonal axis of symmetry. So, for the obtainence of the curve for the core properties, the theory for an hyperelastic material was reviewed from reference [7] and from pages 22-24. Thus, specimens of the core material were created with the dimensions of *Figure 7* and the properties were experimentally determined according to *Table 3*.

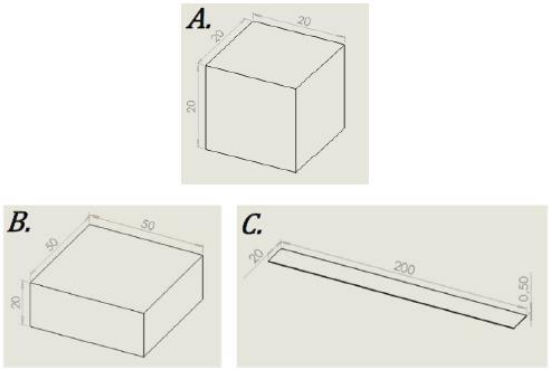


*Figure 7: Specimen's dimensions (in mm) for the compression tests in all directions (A.), for the tensile tests in the radial direction (B.) and for the tensile tests in the tangential and axial directions (C.).*

*Table 3: Standards for the tests using the core's material.*

| Test method | Test Type | Directions |
|---|---|---|
| ASTM C365-03 | Compression | All |
| ASTM C297 / TUB-Shower | Tensile | Radial |
| ASTM D638 | Tensile | Tangential, Axial |

For the experimental properties, experimental tests were performed on an INSTRON machine at 5 mm/min for the compression tests and at 2 mm/min for the tensile. The VIC 2D software was only used for the tensile tests along the tangential and axial directions, since its implementation was hard or impossible on the other tests (*Figure 8*). After the tests and the respective correlations were made, the experimental curves can be obtained and compared with the analytical available data for boiled cork (*Figure 9* and *Figure 10*).

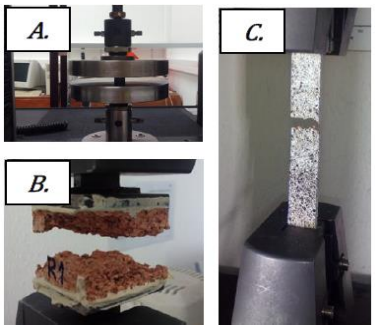


*Figure 8: Specimen after the compression test (A.) and after the tensile test for the radial direction (B.) and for the tangential and axial directions (C.).*

Comparing both, one can see that the hyperelastic behavior under compression persists and it is intensified, since the material can withstand higher compressive loads for the same

compressive strain. Although this behavior can be verified almost throughout the entire curve and for all directions, it is more visible for higher strains. Under tension, even though the addition of resin occurred for the production of agglomerated cork and it would have been expected that its behavior was stiffer and more rigid than the one given for the boiled cork, it can be seen that the slope of the experimental curves are lower, when compared with the analytical curves. Therefore, agglomerated cork can reach higher tensile strain values, when compared to the boiled cork planks, meaning that its behavior is more flexible. Since agglomerated cork is considered on the experimental curve, this will be the only one considered for the FEA (*Figure 11*).

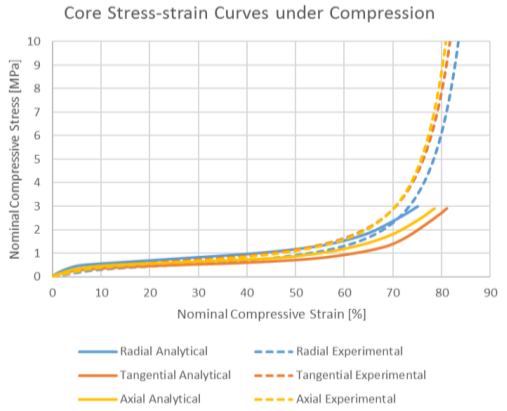


*Figure 9: Stress-strain curves in compression.*

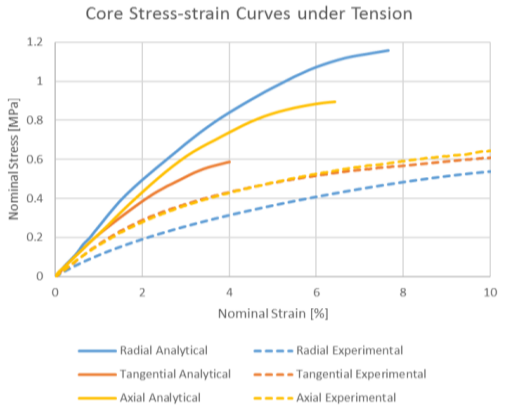


*Figure 10: Stress-strain curves in tension.*

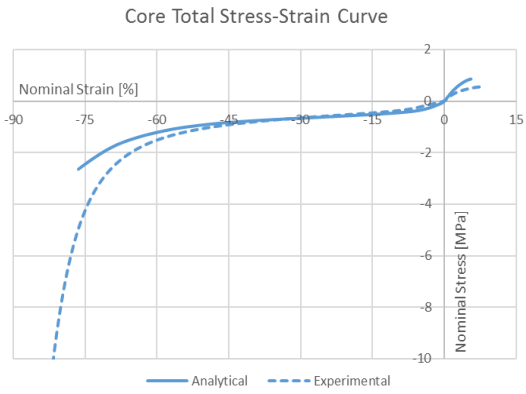


*Figure 11: Stress-strain curves for boiled cork (Analytical) and for agglomerated cork (Experimental).*

### 3.2. Set-up description

The main objective of the experimental compression test is the obtainence of the experimental load-displacement curve. The experimental tests were performed on an INSTRON machine at 2 mm/min, simultaneously with the VIC 3D. Two steel bars of the same width as the panel were produced, to simply support the panel on the tab. Due to the panel's dimensions, both the upper and lower bars were rotated 45º counter clockwise, for the panel to fit the INSTRON machine, while not being in contact with it duration the whole assay. Preliminary panels were tested and, for the curved panels, the best way is to test the panel with the pattern on its convex side, because of the reduced projection errors (*Figure 12*). Since the panel's compression forces its curvature to get bigger, if the pattern is on the convex side, the cameras will capture progressively more focused sets of dots.

*Figure 12: Curved panel during a compression test.*

### 3.3. Experimental compression test results

After the tests were performed for each one of the panels, the results were synchronized by the time correlation program and the final set of points that define the compressive test of each panel could be obtained (*Figure 13*).

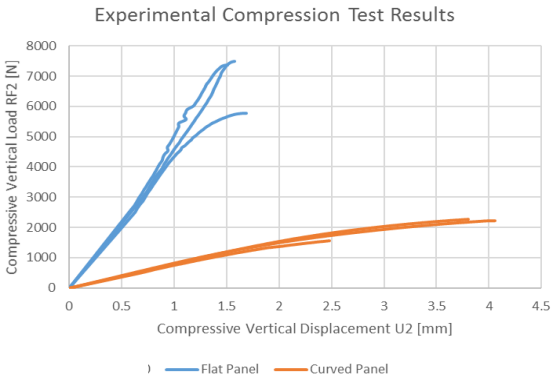


*Figure 13: Experimental curves for the compressive vertical load as a function of the compressive vertical displacement (RF2-U2 curves), for the flat and the curved panels under a compression test.*

The first observed characteristic is that the three tested flat panels have an identical behavior between them, with no relevant discrepancies, fact that also occurs for the three tested curved panels. For all the panels that were tested, due to the skin's fiber and resin characteristics, which strengthen and confer rigidity to the final composite, a purely elastic behavior can be observed. Performing a linear regression on each curve, it is possible to

obtain their expected behavior. It is important to refer that the slope m of these linear curves can also be a measurement of stiffness, even though it does not give directly the Young's Modulus (*Table 4*).

*Table 4: Slope (m) and coefficient of correlation ($R^2$) of the linear regression curves defined for the flat (up) and curved (down) panels under a compression test.*

| Flat | 1 | 2 | 3 | Mean |
|---|---|---|---|---|
| $m$ | 4 682. 09 | 4 981.92 | 3 933.42 | 4 532.48 |
| $R^2$ | 0.988 | 0.984 | 0.911 | - |

| Curved | 1 | 2 | 3 | Mean |
|---|---|---|---|---|
| $m$ | 685.15 | 681.37 | 643.49 | 670.01 |
| $R^2$ | 0.960 | 0.918 | 0.874 | - |

Due to the value of the linear regression curve's slope m, it is possible to verify that the flat panels are circa 6.75 times stiffer than the curved panels. With the introduction of curvature on the panel, its stiffness is progressively reduced, but this might outcome some advantages. Stiffer panels (such as the flat panels) withstand forces more than 6.75 times higher than less stiffer panels (such as the curved panels), but withstand circa 15% of the total displacement withstood by the curved panels.

The third flat panel and the first curved panel have experienced catastrophic failure earlier than the other panels of the same time. On both cases this was mainly due to the production method. For the third flat panel tested, the panel had a bit more warp than the other two, which might have lead to the small discrepancies witnessed. On the other hand, for the curved panel, the first panel had considerably more bubbles and warp, when compared to the other ones produced. Besides that, during the cure on the oven, there was even a local in the middle of the panel that suffered stronger heat effects, when compared to the rest of the panel, which might have reduced the panel's stiffness.

### 3.4. Failure mechanisms

For both the flat and the curved panels, the failure mechanisms and its chronological sequence were identical, even though they can be more easily visualized on the curved panel. When the compressive loads start to be applied, the panel's skins start to slowly wrinkle, phenomena that is more visible on the most fragile skin of the sandwich. Wrinkles on the skins tend to get bigger as the applied compressive loads increases until a point in which the panel's core is crushed by the most fragile skin and local indentation occurs. At this phase, the face in which the most fragile skin crushed the core suffers face failure, in which the direction is approximately parallel to the length of the panel and located approximately in the middle of the panel's width (*Figure 14*). This means that both the composite and the skins thicknesses, as well as the skins strength, were insufficient to withstand the applied compressive load, which led to the panel's face failure.

The face failure occurred always on the face that was under compression, by detriment of the one that was under tension, fact that is justified by the panel's production method, in which a skin tends to always get thicker than the other one. When pressure is applied, by the action of the vertical gravity forces and particularly due to the resin impregnation on the agglomerated cork core, resin tends to infiltrate from the upper skin (where pressure is directly applied) down to the core and eventually reaching the lower skin. Thus, the lower skin will tend to get thicker, but also more fragile than the upper skin, which means that the panel will fracture first on the lower skin (*Figure 14*).

*Figure 14: Face failure visible on the curved panel (left) and section view of the face failure on the most fragile skin (right).*

## 4. Numerical study

For the numerical study of the panels under a compression test, many different FEA software might have been chosen. However, since contact analysis will be needed and since Abaqus is a robust software in terms of performance, Abaqus 6.13® software was chosen.

### 4.1. Materials

For the numerical model, three materials were defined.

The material of the bars is steel, whose properties were taken from the steel manufacturer tables [11] at page 16. The density is 7 850 kg/m$^3$ and the behavior is elastic and isotropic, with a Young's modulus of 200 GPa and a Poisson's ratio of 0.3, as most steels before yield [11].

For the composite's core, the density is 200 kg/m$^3$, obtained from the manufacturer tables [12], and the behavior is hyperelastic and isotropic. A Poisson's ratio of 0.15 was chosen, since it varies with the level of deformation on compressed cork agglomerates, from 0.15 on the beginning, to around 0.05 and rising up after densification takes place [13]. The hyperelastic model that has the best correlation with the experimental curve is the fifth order Ogden's strain energy potential (*Figure 15*). Some available models diverged and are not represented. The Ogden model is the generalization

of the Mooney-Rivlin and Neo-Hookean models. From Abaqus 6.13® Analysis User's Guide [14]:

$$U = \sum_{i=1}^{N} \frac{\mu_i}{\alpha_i^2}\left(\bar{\lambda}_1^{\alpha_i} + \bar{\lambda}_2^{\alpha_i} + \bar{\lambda}_3^{\alpha_i} - 3\right) + \sum_{i=1}^{N} \frac{1}{D_i}(J-1)^{2i} \quad (1)$$

, where the parameter $N$ is 5, $\mu_i \alpha_i > 0,\ \forall i = 1, \dots N$ (no sum over $i$), $\sum_{i=1}^{N} \mu_i \alpha_i = 2G, \forall G > 0$, $G$ is the Shear Modulus, $D_i$, $\mu_i$ and $\alpha_i$ are material parameters, $J$ is the elastic volume strain and $\bar{\lambda}_i$ are the principal stretches of the Cauchy-Green tensor.

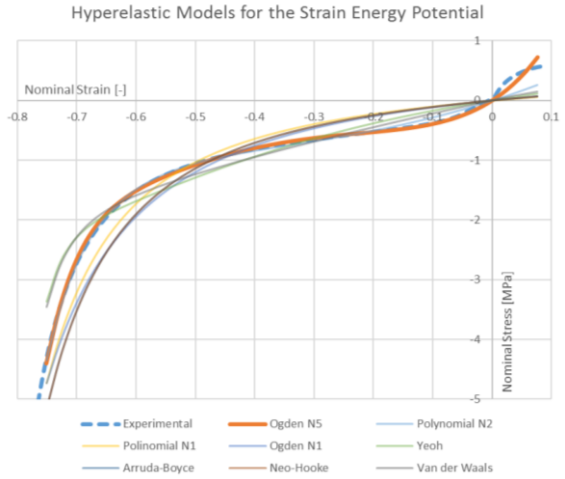


*Figure 15: Fitting of the hyperelastic models with the experimental test data curve. The Ogden N5 curve is the one that best fits the Experimental curve.*

For the composite's skins, the density is 1 169 kg/m$^3$, obtained analytically, and the behavior is elastic and orthotropic (but transversally isotropic). The engineering constants, i.e., the nine independent material coefficients for an orthotropic material ($E_1$, $E_2$, $E_3$, $G_{23}$, $G_{13}$, $G_{12}$, $\nu_{12}$, $\nu_{13}$, $\nu_{23}$), were introduced. The material orientation is at *Figure 16*.

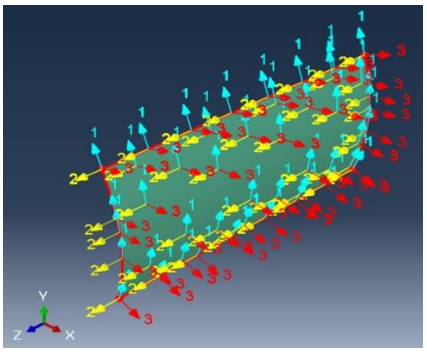

*Figure 16: Material orientation axes, as seen in Abaqus for the curved panel.*

### 4.2. Interaction and loading conditions

The flat panels and bars are considered as homogeneous solids and the curved panels as homogeneous shells.

When assembled, the interaction between the skins and the core of the composite must be defined, being the steel bars defined as rigid bodies and the skins tied with the composite's core. For the interaction between the steel bars with the total panel, a surface-to-surface contact exists. For this contact property, the normal and the tangential behaviors must be defined. For the normal behavior, hard contact and no separation after contact were the options selected. For the tangential behavior, tangential or friction forces must be considered. Since the data found in the literature may vary significantly, the value used for the friction coefficient was 0.5, obtained for the dry friction of a steel-wood interface [15].

As for the loading conditions, for both the up and the bottom bars, all six degrees of freedom were fixed. However, and only for the top bar, the vertical axis was not fixed and a displacement of -200 was introduced. This value is negative since, according to the global axis, it will compress the panel.

### 4.3. Finite elements mesh

For the finite elements mesh, a continuum shell element was considered for the panels and a 3D stress element was considered for the bars. The approximate global seed size was chosen and this value was changed, to verify the convergence of the FEA. The size of the elements for the most refined meshes was 5 mm (*Figure 17*). Meshes with smaller elements, due to the high allocation of memory requested from the CPU, could not be simulated.

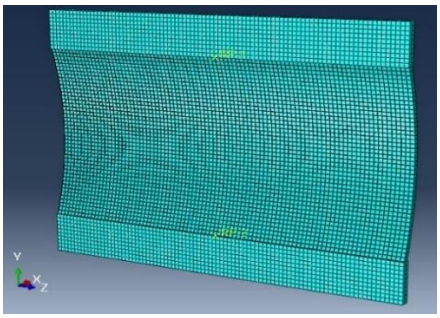

*Figure 17: Finite elements mesh with 5 mm of size, as seen in Abaqus for the curved panel, under a compression test.*

### 4.4. Type of analysis

A physically and geometrically non-linear static analysis was performed. When only material instability exists, the General static analysis is enough. However, when geometric instability also exists, Riks static analysis is best suited due to its arc-length method. Thus, Riks static analysis was chosen since it can process the decreasing part of the load-deformation curve (i.e., for zero and negative stiffness), while the General static analysis will diverge in this case.

### 4.5. Numerical compression test results

After the finite elements analysis, its accuracy was verified through a convergence study, were the mesh size was changed from elements with 100 mm under to elements with 5 mm. For both panels, since the behavior of the vertical displacement (U2) and vertical load (RF2) curve converges to a specific

curve when the mesh size is increasingly more refined, convergence is verified (*Figure 18* and *Figure 19*). Due to the curved panel's geometry that increases non-linear effects, the computational time requested for the curved panel's FEA is more than the one requested for the flat panel's.

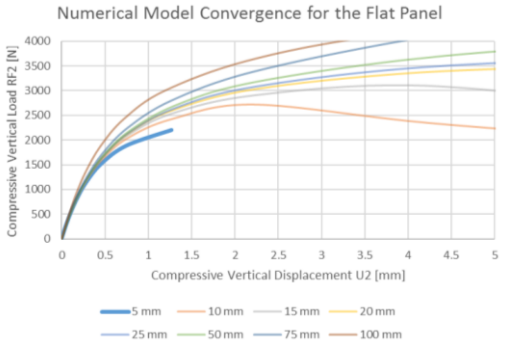


*Figure 18: Convergence verification for the flat panel's numerical model, where the FE size was reduced from 100 mm to 5 mm.*

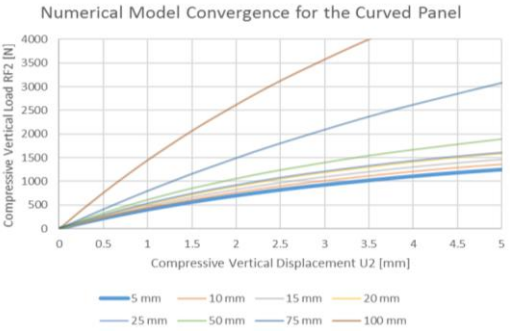


*Figure 19: Convergence verification for the curved panel's numerical model, where the FE size was reduced from 100 to 5 mm.*

When a linear regression is performed, considering only the first 0.3 mm of the compressive vertical displacement (U2) to raise accuracy, one can conclude from the coefficient of determination ($R2$) that the linear regression is valid. *Table 5* presents the value of the slope $m$ and the coefficient of correlation $R2$, considering both panels and the experimentally (index 'A') and the analytically (index 'B') determined properties for the skins.

*Table 5: Slope ($m$) and coefficient of correlation ($R2$) of the linear regression curves for each panel and for a compression test, considering the most refined mesh. The experimental (column A) and the analytical (column B) properties for the skins were studied.*

| | Flat Panels | | Curved Panels | |
|---|---|---|---|---|
| | *A* | *B* | *A* | *B* |
| $m$ | 4 181.23 | 4 660.98 | 440.43 | 478.04 |
| $R^2$ | 0.981 | 0.973 | 0.999 | 0.999 |

### 4.6. Comparison between the experimental and the numerical results

*Figure 20* presents a comparison between the experimental and the numerical results regarding the compression tests on both the flat and the curved panels, with the experimentally and the analytically determined properties for the skins. Considering the experimental results as reference for the relative error, with the $m$ values of the A columns of *Table 5*, the relative error is 7.75% for the flat and 34.27% for the curved panel and, with the $m$ values of the B columns, the value is 2.83% for the flat and 28.65% for the curved panel.

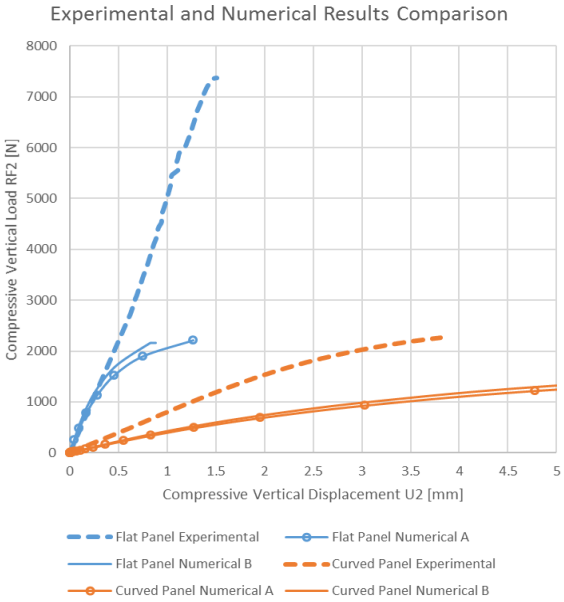


*Figure 20: Comparison between the linear regression of the experimental and the numerical curves for the compressive vertical load as a function of the compressive vertical displacement (RF2-U2 curves), obtained for both panels.*

The results obtained using the analytical properties for the skins are always more accurate than the ones obtained with their experimental properties, since the panels simulated numerically with the analytical properties for the skins correspond to the purely analytical result and, since the FE program usually is more rigid than the reality, when the experimental properties for the skins are introduced, the slope of the linear curve is lower (as expected), which means that the panel is less rigid. Nonetheless, the slope of the linear regression for the results of the flat panels experimentally tested, has a value in the middle of both numerical results. However, for the curved panels, it is higher than for both numerical results.

Two major reasons influence this behavior, which only occur experimentally and cannot be properly simulated: the resin impregnation on the cork core and the warp of the panels. During the production method and the cure process, the resin that was laid on the skins flows from them to the cork core, which then tends to get stronger. Thus, the rigidity of the panel increases, as well as the slope of the linear regression, being this a characteristic experienced by both the flat and the curved panels. Considering now the warp of the panels, this effect always occurs when a structure of

this type is produced. When a panel is curved, the warp will not have as much impact on it during a compression test, as it has when a panel is flat, almost only due to the geometry of the structure. Thus, the warp will decrease both panels rigidity. However, this decrease is way more significant on the flat panel, which will place the slope of the experimental linear regression on the middle of the other two numerical linear regressions.

Therefore, the numerical models correctly reproduced the experimental results in terms of initial linear elastic stiffness and initial non-linear behavior. However, when the non-linear behavior is simulated for larger displacements, the numerical model loses accuracy.

Comparing the experimental and numerical failure mechanisms, one might observe that for both panels the behavior is somewhat similar. However, and particularly for the flat panel, the experimental failure mechanism tends to occur in one specific line located in the middle of the panel (which is not perfectly straight), whereas the numerical failure mechanism tends to occur in two parallel lines, located at the same distance from the middle of the panel. This difference is justified particularly because the experimental system is far from being perfect, which means that the experimental failure occurs due to microfractures on the panel's skins which tend to propagate and ultimately lead to the face failure along one roughly straight line. On the other hand, on the numerical FEA, the numerical failure occurs on the specific spots in which the maximum moments are generated, that correspond to the two referred lines.

## 5. Conclusions

Planar and non-planar panels, with epoxy and glass fibers skins and agglomerated cork core, were tested experimentally and simulated numerically.

### 5.1. Achievements

On an early stage of this study, experimental tests were performed. First, the mechanical properties of both the skins and the core material were determined, when the material was subjected to different types of solicitations, following the applicable standards for the effect. The results were compared with the available analytical solutions and the determined properties are according to what was expected, i.e., the skins are orthotropic and the core is isotropic. The discrepancies that exist between the experimental and the analytical solutions are explained by the method of production and by the mean strains given by the VIC software.

After the determination of the properties, the mechanical behavior of the total sandwich structure was experimentally tested. Flat and curved panels were produced and they were subjected to compression tests. The flat panels were proved to be 6.75 times stiffer than the curved panels, while withstanding only circa 15% of the displacement withstood by the curved panels. Also, both the flat and the curved panels presented the same sequence of mechanisms until their catastrophic failure.

For the numerical model, it was progressively developed until its final configuration. Its analytical and experimental properties for the materials were inserted, border conditions and interactions between the parts were defined and the FEA was performed. With the available software's functions, it is impossible to proper and accurately simulate the complete non-linear mechanical behavior of agglomerated cork, used as core of the sandwich. Furthermore, the author of this study states that this conclusion can be generalized to other materials whose behavior is similar to agglomerated cork, such as wood or bone, since they are hyperelastic and non-linear materials and, particularly and mainly, since they are cellular. Natural materials present random effects which are hardly to predict by the FE software. But, for small displacements, the analysis using Abaqus can be considered as accurate for engineering purposes and the numerical model is valid, even though the correlation between the experimental and the numerical results is not as perfect for the curved panel as it is for the flat, which is mainly due to its geometry. Using the available models provided by Abaqus and considering agglomerated cork, the best hyperelastic model that fits the experimental data is the fifth order Ogden's strain energy potential. The software is unable to accurately account for the resin impregnation from the skins to the core, which means that the real experimental core properties are different from the ones introduced and simulated by the FE software.

From the compression test, the numerical results obtained using the analytical properties for the skins are always more accurate than the ones obtained with their experimental properties. The panels with the analytical properties for the skins correspond to the purely analytical result and, since FE software are more rigid than the reality, when the experimental properties are introduced, the slope of the linear curve is lower, which means that the panel is less rigid. When using the experimental properties for the skins, the resin impregnation and the warp of the panels play an important role. Resin impregnation increases the rigidity of the panel, as well as the slope of the linear regression, which occurs for both panels. However, when warping on a curved panel is considered, the warp will not have as much impact on it during a compression test, as it as when a panel is flat. Even though the warp of the panels decreases their rigidity, this decrease is way more significant on the flat panel.

The obtained results show the potential of numerical models to characterize the mechanical behavior of these type of sandwich structures with cellular and non-linear cores, as a mean of validation of experimental data and, furthermore, as an alternative to the experimental tests themselves.

### 5.2. Further developments

The extensive study herein justifies the following future developments on the topic:

- The panel's production method could be improved, since one skin of the panel tends to always get thicker than the other one. Besides this, effects such as the fibers misalignment, the amount of measured resin and warping lead to differences between the experimental and the numerical results.
- The analysis using VIC could be improved. The mean strain values sometimes appear noisy and with high projection error values. The brightness of the images, the variation of the pattern and the presence of hot light sources have an important role on their accuracy. Though these effects were minimized, further tests should be made to reduce them to their almost completely elimination.
- The numerical model could also be improved. A stochastic model for the resin impregnation on the agglomerated cork core should be created using Fortran and then inserted on the numerical model. This stochastic model would not be purely, but partially stochastic, since some variables present a fixed behavior, while others must be classified as non-deterministic, since their behavior can only be determined based on experimental results.
- A small-scale test correlation could be made.
- A parametric study on the best curvature configuration for the panel to be used on the referred application would also be of interest.

Finally, while this study focused on the mechanical characterization of a non-planar sandwich panel with agglomerated cork core, the proposed technology holds great promise for the implementation on aircraft and for their potential implementation on other types of applications.

## 6. Acknowledgements

The author would like to thank its supervisors Prof. Pedro Amaral and Prof. Nuno Silvestre, who provided the opportunity to work at Instituto Superior Técnico (IST) and at Frontwave Stone Technology (FW), for their support and advice; to Eng. Joel Pinheiro and the team at FW, for accepting my research; to Almadesign, for providing the documents regarding the DesAIR Project; to all the professors and colleagues at IST, for the help throughout this research; and, last but not least, a special thank to the author's family, girlfriend and friends, for being always there unconditionally.

## 7. References

[1] Silva, S. P.; Sabino, M. A.; Fernandes, E. M.; Correlo, V. M.; Boesel, L. F.; Reis, R. L.; "Cork: properties, capabilities and applications"; *International Materials Reviews* vol.50 no.6 (2005): 345-365.

[2] Inwood, S.; *The Forgotten Genius: The Biography of Robert Hooke 1635-1703*; San Francisco, CA: Macadam Cage Pub, 2005.

[3] Costa, A.; Pereira, H.; "Caracterização e Análise de Rendimento da Operação de Traçamento na Preparação de Pranchas de Cortiça para a Produção de Rolhas"; *Silva Lusitana* vol.12 no.1 (2004): 51–66.

[4] Mourão, T.; *Extraction of added value products from black condensate*; 2012.

[5] Pereira, H.; *Cork: Biology, Production and Uses*; Lisbon: Elsevier Science, 2007.

[6] DesAIR Consortium, Design of Environment Friendly Structures for Aircraft [Online]. Available: desair.inegi.up.pt [07-Mar-2016].

[7] Reddy, J. N.; *Mechanics of Laminated Composite Plates and Shells - Theory and Analysis*; Boca Raton, FL: CRC Press, 2nd edition; 2004.

[8] Resoltech, Resoltech 1050 Resin [Online]. Available: resoltech.com [04-Apr-2016].

[9] HexForce, 7725 Product Data [Online]. Available: hexcel.com [22-Nov-2016].

[10] Walleberger, F. T.; Watson, J. C.; Li, H.; "Glass Fibers"; *ASM Handbook Composites* vol.21 no.19 (2001): 27-34.

[11] A. Series, Stainless Steel: Tables of Technical Properties [Online]. Available: worldstainless.org [06-Oct-2016].

[12] Amorim Cork Composites, *Technical Data Core Cork*, 2009.

[13] Jardin, R.; Pereira, A. B.; "Static and dynamic mechanical response of different cork agglomerates"; Elsevier Materials and Design vol.68 (2015): 121-126.

[14] Abaqus 6.13 Analysis User's Guide [Online]. Available: 129.97.46.200:2080 [06-Nov-2016].

[15] Johnston, B.; Cornwell, M.; Beer, F. P.; *Vector Mechanics for Engineers Statics and Dynamics*; New York, NY: McGraw-Hill, 9th edition; 2010.